Phase diagram of ternary mixtures water + *n*-alkane + non-ionic surfactant

Hiroyuki Matsuda*[,1], Yuki Nakazato[1], Rei Tsuchiya[1], Yoshihiro Inoue[1], Kiyofumi Kurihara[1], Tomoya Tsuji[2], Katsumi Tochigi[1], Kenji Ochi[1]

[1] Department of Materials and Applied Chemistry, Nihon University, 1-8-14 Kanda Surugadai, Chiyoda-ku, Tokyo 101-8308, Japan
[2] Malaysia-Japan International Institute of Technology, Universiti Teknologi Malaysia, Off Jalan Sultan Yahya Petra, Kuala Lumpur 54100 Malaysia

* To whom correspondence should be addressed.
E-mail : matsuda.hiroyuki@nihon-u.ac.jp Tel : +81-3-3259-0814 FAX : +81-3-3293-7572

Abstract

The object of this work is an accurate determination of the phase diagram of ternary mixtures water + *n*-alkane + *n*-alkyl polyglycol ether (C_iE_j) using a cloud point method with laser scattering technique. *n*-Octane and *n*-dodecane were selected as *n*-alkane. 2-butoxyethanol (C_4E_1) and 2-(2-hexyloxyethoxy)ethanol (C_6E_2) were selected as non-ionic surfactant. In the measurements of ternary mixtures, the C_iE_j free basis mass fraction of *n*-alkane "α" was changed from 0.1 to 0.9. In the fish-type phase diagram, body is three-liquid phase, tail is one-liquid phase, and another region is two-liquid phase. An intersection of the body and tail is called "X-point". Changes in the phase diagram and X-points with different *n*-alkane, C_iE_j, and the value of α were discussed from the experimental data.

Keywords

Non-ionic surfactant, Phase equilibria, Fish-shaped

1. Introduction

n-Alkyl polyglycol ethers $CH_3(CH_2)_{i-1}(OCH_2CH_2)_jOH$ (C_iE_j) are the most important class of non-ionic surfactants. They are widely used in many different industrial processes such as the surfactant flooding in tertiary oil recovery, production of herbicides, drugs, cosmetics and nano particles [1, 2]. Non-ionic surfactants are generally more expensive than other surfactants. Especially in the surfactant flooding process, one must minimize the consumption of non-ionic surfactants and maximize the recovery of residual oil. Thus, understanding the phase equilibria

of the ternary mixture water + alkane + C_iE_j is very crucial to know the optimal conditions in the flooding process [3]. It is also important in the fundamental research of critical phenomena and wetting transitions [4]. Phase diagram of water + alkane + C_iE_j has been reported to exhibit complex behavior called "Fish-Shaped", when the temperatures of phase transitions are plotted vs. the mass fraction of C_iE_j in the fixed water / alkane mass ratio. Especially, an intersection of the body and tail of the fish-typed phase diagram is called as "X-point". According to Winsor nomenclature [5], X-point is the intersection at which the one-phase Winsor (Winsor IV), the two-phase (Winsor I and II), and three phase (Winsor III) regions meet. X-point corresponds to the minimal surfactant concentration required to obtain a one-phase microemulsion (Winsor IV). So, it is important to choose a suitable surfactant and surfactant concentration in the processes using the surfactant.

On the other hand, Wade et al. introduced the equivalent alkane carbon number (EACN) [6]. It is a dimensionless number and shows the hydrophobicity of oil. The EACN value of a given oil is equal to the number of carbons the *n*-alkane exhibiting the same phase behavior. Many reliable EACN values have been determined for various type of oils such as triglycerides [7], aliphatic or aromatic hydrocarbons [8, 9], ether or esters [10, 11], and terpenes [12]. The EACN concept is particularly interesting not only for applications in perfumery, cosmetic, pharmaceutical, etc., but also from a molecular point of view due to exhibiting a wide range of chemical structures such as acyclic, mono- or polycyclic, cycles of different sies, branched, unsaturated [13]. Determination of reliable values of EACN has been done by so called fishtail method based on the experimental temperature in the X-point and the fish-shaped diagram of well-defined ternary systems water + oil + C_iE_j [9].

Over the past decades, a considerable amount works has been done to investigate the phase behavior of the mixtures water + alkane + C_iE_j [3, 14-23]. Especially, the fish-typed phase diagrams of the ternary mixtures water + alkane + C_iE_j have been investigated by several research groups [3, 15-17, 20-23]. These previous measurements are mainly basis on the visual method for the observation of the phase change. Queste et al. [9] used the visual determination of the fishtail diagram based on the ability to scatter the light of a laser pointer. On the other hand, our group have developed a new laser light scattering technique for measuring mutual solubility curves for easy and accurate determination of liquid-liquid equilibrium (LLE) data [24]. We have previously used this technique to measure the LLE for binary mixtures [25-32]. If this experimental apparatus and procedure could be applied to the measurements of the fish-typed phase diagram including the X-point, rapid and accurate measurements of them could be achieved. Also, it would lead a determination of reliable values of EACN.

This work aims for an accurate determination of the fish-shaped diagrams for ternary mixtures water + *n*-alkane + C_iE_j using a cloud point method with a laser-scattering technique. *n*-Octane and *n*-dodecane were selected as *n*-alkane. 2-butoxyethanol (C_4E_1) and 2-(2-

hexyloxyethoxy)ethanol (C_6E_2) were selected as non-ionic surfactant. In these measurements, the C_4E_1 or C_6E_2 free basis mass fraction of *n*-octane or *n*-dodecane "α" was changed from 0.1 to 0.9. In the mixture water + *n*-octane + C_4E_1, the phase diagram at the C_4E_1 free basis mass fraction of *n*-octane, α = 0.5, have been reported by Andersen et al. [3] Thus, firstly, the experimental apparatus and procedures of the fish-shaped diagrams were verified by comparing our experimental data with the literature values. X-points were determined from the experimental LLE data. Changes of the fish-typed phase diagram according to the value of α and the carbon number of C_iE_j was discussed.

2. Experimental

2.1. Materials

The chemicals used in this work are summarized in Table 1. The purities of the materials were checked by gas chromatograph (GC-4000, GL Sciences Co., Ltd., Tokyo, Japan) with a thermal conductivity detector. The water contents of all chemicals except water were checked using a Karl Fischer moisture meter (CA-200, Mitsubishi Chemical Co., Ltd., Tokyo, Japan). The densities (ρ) at 298.15 K were measured using a precision digital Anton Paar oscillating u-tube densimeter (DMA 4500) with a reproducibility of 10^{-2} kg m^{-3}. Experimental ρ at 298.15 K of the chemicals used in this work are shown in Table 2 together with the literature values [34].

Table 1

Chemicals used in this work.

Component	CAS Registry Number	Source	Purification method	Purity (mass fraction)	Water content (ppm)
Water	7732-18-5	Distillated water made in laboratory	No	-	-
n-octane	111-65-9	Wako Pure Chemical Industries	Molecular sieves 4A	0.998	12
n-dodecane	112-40-3	Wako Pure Chemical Industries	Molecular sieves 4A	0.998	23
C_4E_1 [a]	111-76-2	Wako Pure Chemical Industries	Molecular sieves 4A	0.997	73
C_6E_2 [b]	112-25-4	Wako Pure Chemical Industries	Molecular sieves 4A	0.993	85

[a] IUPAC name: 2-butoxyethanol

[b] IUPAC name: 2-(2-hexyloxyethoxy)ethanol.

Table 2

Densities at 298.15 K, ρ at 298.15 K used in this work.

Component	ρ (298.15 K) (kg m^{-3}) [a]	
	Experimental	Literature [b]
Water	997.07	997.05
n-octane	698.35	698.62
n-dodecane	745.28	745.18
C_4E_1	896.16	896.25
C_6E_2	928.89	928.93

[a] At P = 101 kPa. Standard uncertainties are $u(\rho)$ = 0.01 kg·m^{-3}, $u(T)$ = 0.01 K, and $u(P)$ = 1 kPa.
[b] Ref. [34]

2.2. Apparatus and Procedure

The fish-shaped diagrams of for ternary mixtures water + *n*-octane + C_4E_1 or C_6E_2, water + *n*-dodecane + C_6E_2 were determined by a cloud point method with a laser-scattering technique. Details of the apparatus and its procedure have been previously described [24, 25]. The light sensor was placed on the position different from the way of light beams so that the weak scattered light appearing at the beginning of formation (or disappearance) of turbidity could be effectively detected. The temperatures of a solution and the intensity of the scattered light were pursued by a computer via the data logger. Temperature control was done with a cooling media. Temperatures were measured with a platinum resistance thermometer (accuracy within ± 0.01 K). In our previous works, the cloud point temperature was determined by a difference of the intensity of the scattered light between one and two liquid phases. Ternary mixtures investigated in this work form not only one and two liquid phases, but also three liquid phases. Fig. 1 shows a sample of the intensity of scattered light vs. temperature between two and three phases in the ternary mixture water (1) + *n*-octane (2) + C_4E_1 (3). The cloud point temperature between two and three phases could be also detected, using the differences of the intensity of the scattered light. The liquid mass fraction was determined gravimetrically (digital balance model AX 504, Mettler Toledo, Columbus, OH, with a sensitivity of 0.1 mg and a maximum load of 510 g).

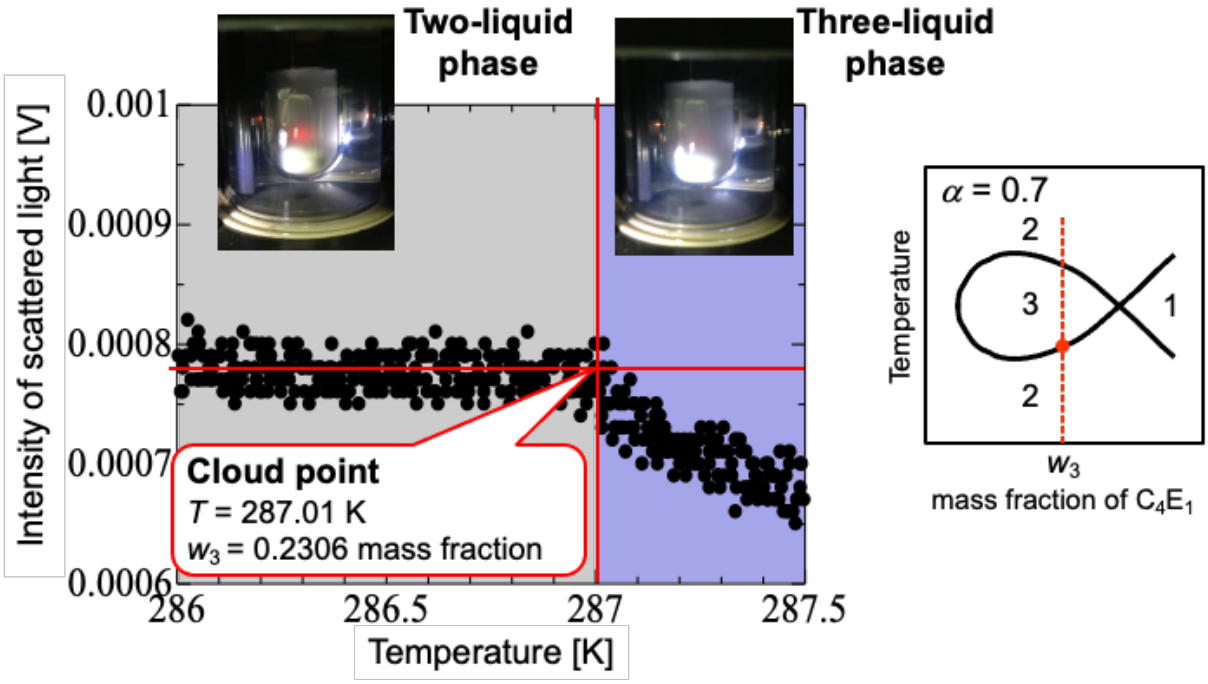

Fig. 1. Intensity of scattered light vs. temperature of solution for the mixture water (1) + *n*-octane (2) + C_4E_1 (3) (w_3 = 0.2306 mass faction)

3. Results and discussion

3.1. Water + n-octane + C_4E_1 or C_6E_2

In the ternary mixture water (1) + *n*-octane (2) + C_4E_1 (3), the phase diagram at the C_4E_1 free basis mass fraction of *n*-octane, α = 0.5, have been reported by Andersen et al. [3] Thus, firstly, the experimental apparatus and procedures of the fish-shaped diagrams were verified by comparing our experimental data with the literature values. The experimental fish-shaped diagram at α = 0.5 for this mixture are compared with the literature values in Fig. 2. "1", "2", " $\bar{2}$", and "3" in Fig. 2 indicate the number of liquid phase [35]. The region "2" is O/W (Oil in Water) microemulsion phase, and the region " $\bar{2}$" is W/O (Water in Oil) microemulsion phase. "1", "2", " $\bar{2}$", and "3" corresponds to Winsor IV, I, II, and III, respectively. Reasonable agreements could be obtained between the experimental and literature values. Therefore, the experimental apparatus designed in this work was applied for the measurements of the fish-shaped diagram.

Figs. 3 and 4 show the experimental phase diagrams with several values of α, 0.1, 0.3, 0.5, 0.7, and 0.9 for the systems water + *n*-octane + C_4E_1 or C_6E_2, respectively. X-points were determined from the cloud points in the vicinity of the intersection of four regions of "1", "2", " $\bar{2}$", and "3" mentioned above. These mass fractions of C_4E_1 or C_6E_2, w_3, and temperatures T are summarized in Table 3. In the fish-type phase diagram, body is three-liquid phase, tail is two-liquid phase, and another region is one-liquid phase. A comparison of the phase diagram

in five values of α is also illustrated in Figs. 5 and 6. The temperature in X-point increases with increasing α. Also, the mass fraction of C_4E_1 or C_4E_6, w_3 shifts to higher concentration up to α = 0.3 (C_4E_1) or α = 0.5 (C_6E_2), and then w_3 decreases considerably in α = 0.9. Behavior of the X-point with an increase of α agreed well with one of the literature data of the mixture water + *n*-decane + C_8E_3 [14]. Temperature range of the three-liquid phase is almost same. However, minimum area was observed in α = 0.9.

Comparisons of the fish-shaped diagrams between the systems water + *n*-octane + C_4E_1 and water + *n*-octane + C_6E_2 at α = 0.5 and α = 0.7 are graphically given in Fig. 7. When the C_iE_j was changed from C_4E_1 to C_6E_2, the phase diagram and X-point shifted to lower temperature and lower concentration of C_iE_j.

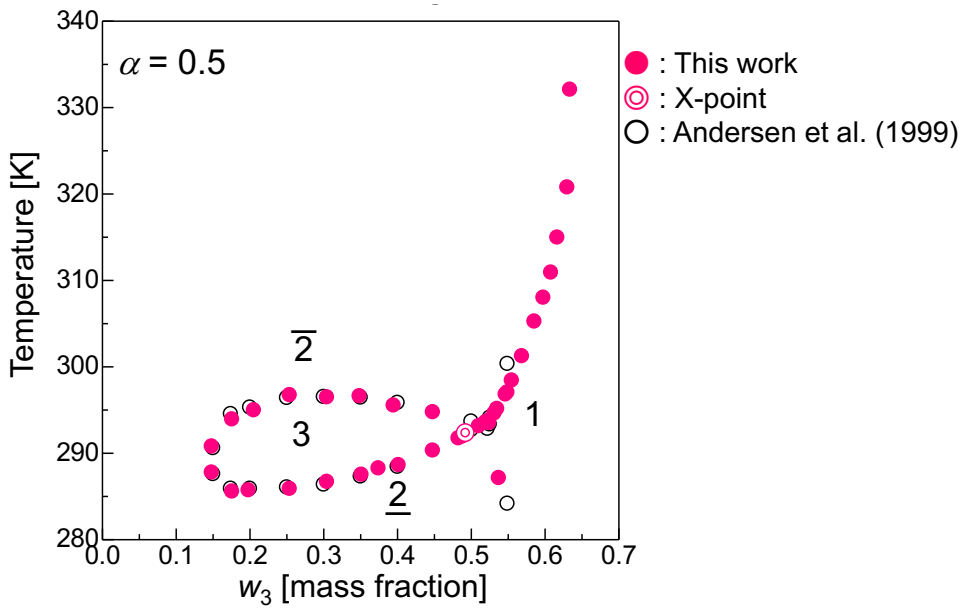

Fig. 2. Experimental fish-shaped diagram for the system water (1) + *n*-octane (2) + C_4E_1 (3).

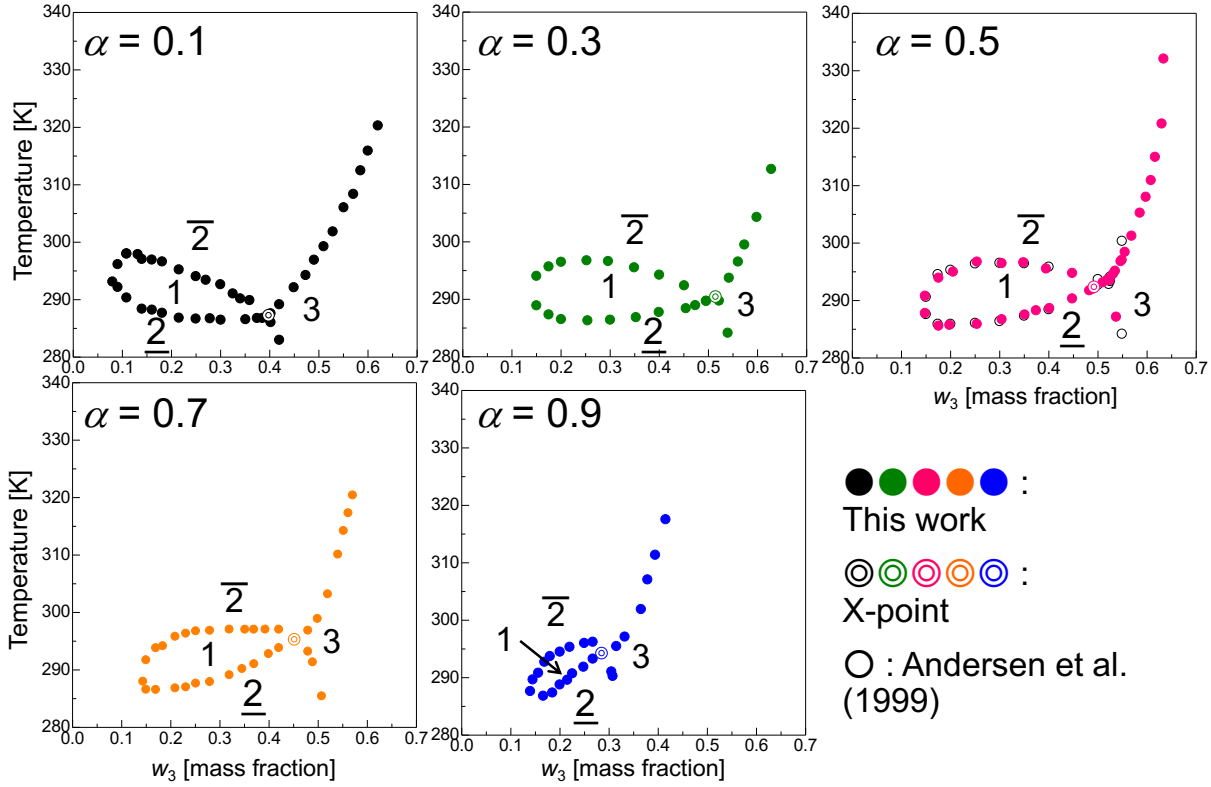

Fig. 3. Experimental fish-shaped diagram for the system water (1) + *n*-octane (2) + C_4E_1 (3).

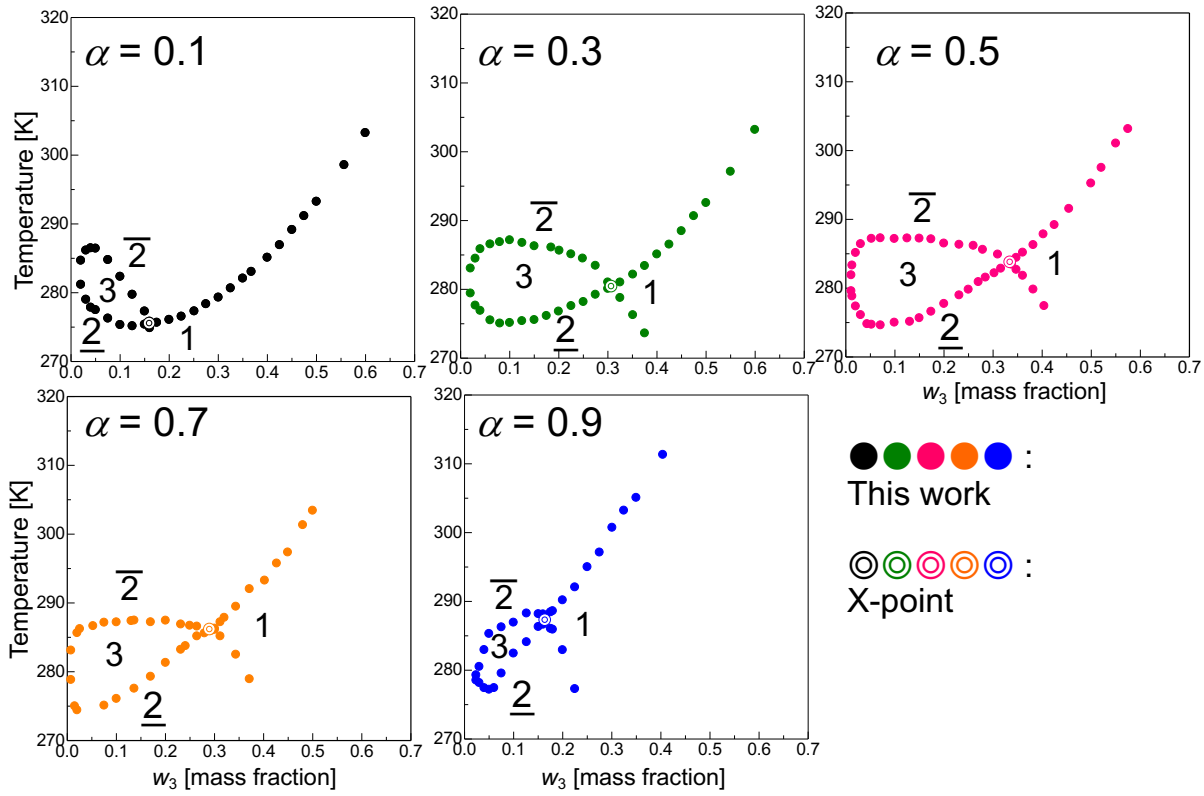

Fig. 4. Experimental fish-shaped diagram for the system water (1) + *n*-octane (2) + C_6E_2 (3).

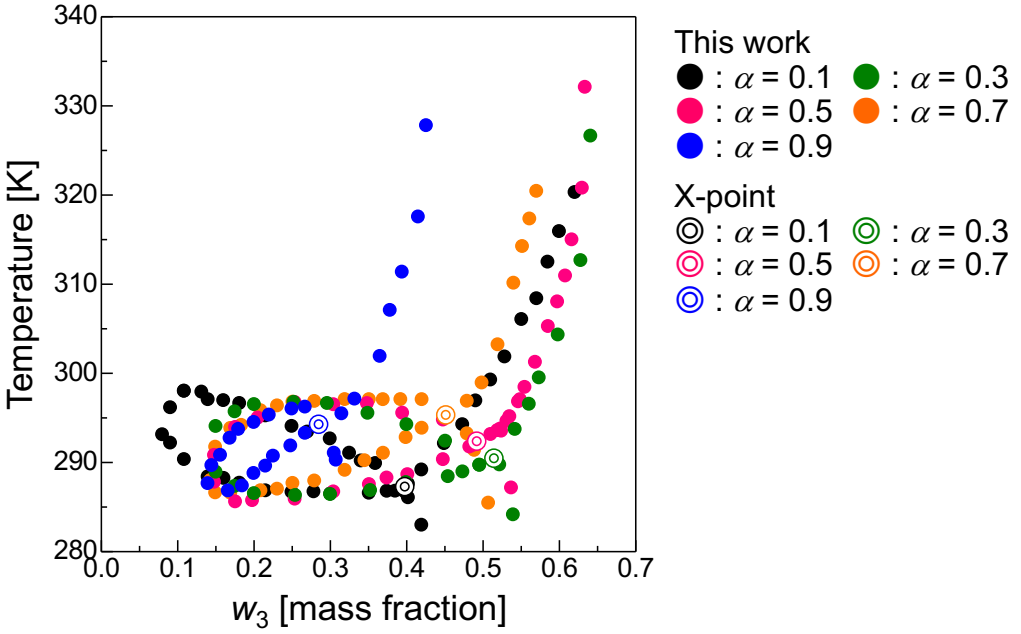

Fig. 5. Experimental fish-shaped diagram for the system water (1) + *n*-octane (2) + C_4E_1 (3).

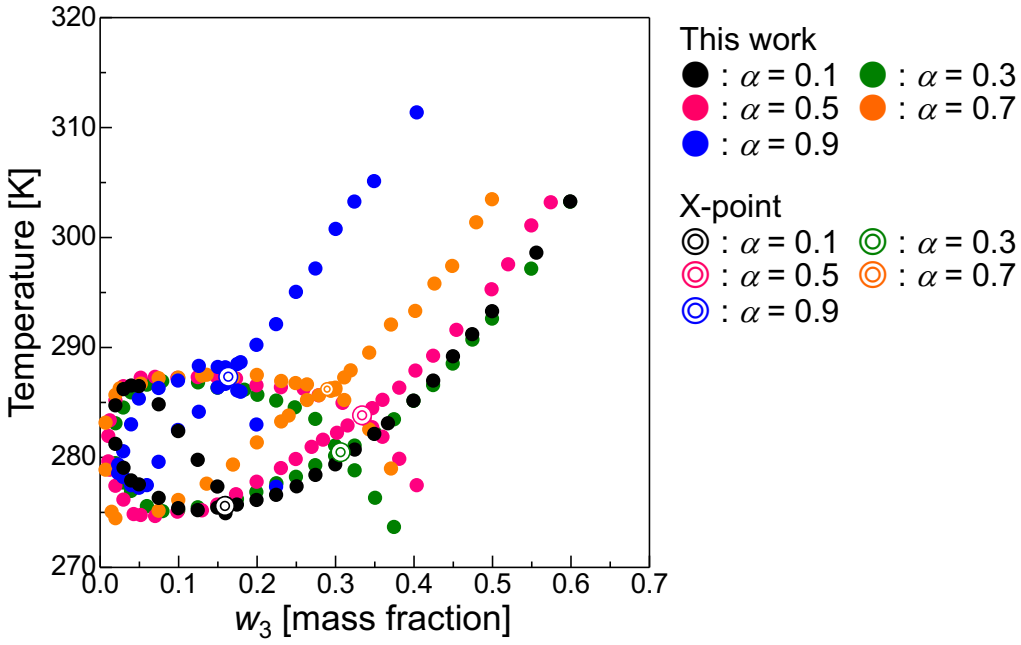

Fig. 6. Experimental fish-shaped diagram for the system water (1) + *n*-octane (2) + C_6E_2 (3).

Table 3

Mass fractions w_3 and temperatures T of X-points for the systems of water (1) + *n*-octane (2) + C_4E_1 (3), water (1) + *n*-octane (2) + C_6E_2 (3), and water (1) + *n*-dodecane (2) + C_6E_2 (3). Standard uncertainties are $u(w_3) = 0.0001$, $u(T) = 0.1$ K.

water (1) + *n*-octane (2) + C_4E_1 (3)			water (1) + *n*-octane (2) + C_6E_2 (3)		
α	w_3 (mass fraction)	T (K)	α	w_3 (mass fraction)	T (K)
0.1	0.3980	287.24	0.1	0.1597	275.54
0.3	0.5148	290.42	0.3	0.3070	280.43
0.5	0.4923	292.33	0.5	0.3344	283.78
0.7	0.4517	295.28	0.7	0.2899	286.16
0.9	0.2852	294.23	0.9	0.1639	287.29

water (1) + *n*-dodecane (2) + C_6E_2 (3)		
α	w_3 (mass fraction)	T (K)
0.1	0.2377	282.40
0.3	0.4309	293.43
0.5	0.4609	298.72
0.7	0.4163	305.09
0.9	0.2263	306.55

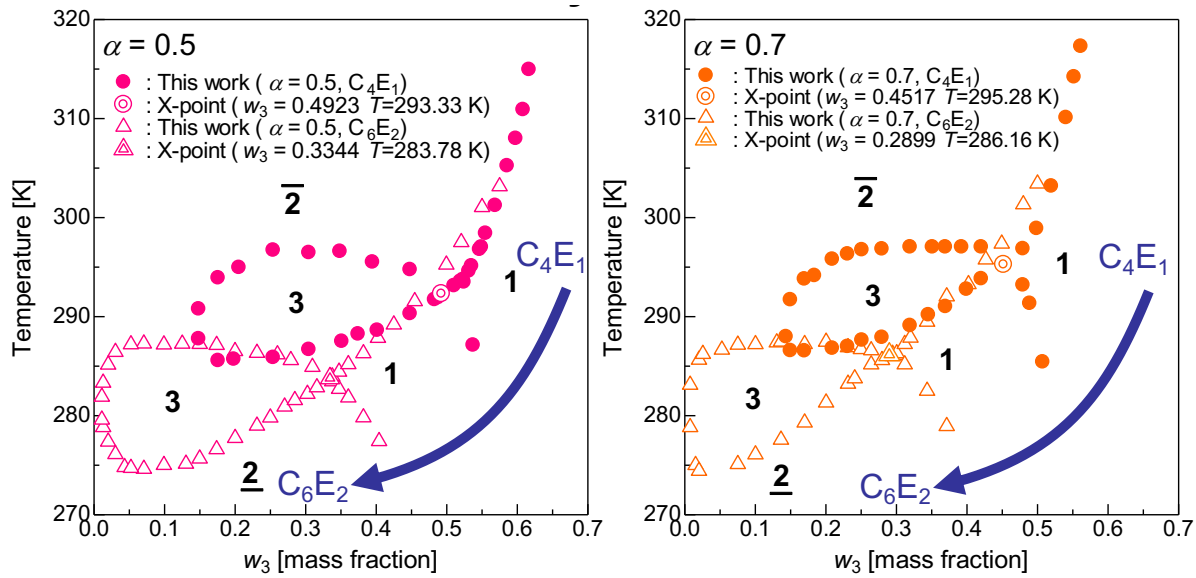

Fig. 7. Comparison of the experimental fish-shaped diagram for the systems water (1) + *n*-octane (2) + C_4E_1 or C_6E_2 (3).

3.2. Water + n-dodecane + C_6E_2

Fish-shaped diagrams of the system water + *n*-dodecane + C_6E_2 with $\alpha = 0.1, 0.3, 0.5, 0.7,$

and 0.9 were also determined. Fig. 8 and 9 show the experimental phase diagrams of this system. Determined mass fractions of C_6E_2, w_3, and temperatures T of X-points are also listed in Table 3. Comparisons of the fish-shaped diagrams between the systems water + *n*-octane + C_6E_2 and water + *n*-dodecane + C_6E_2 at $\alpha = 0.5$ and $\alpha = 0.7$ are also shown in Fig. 10. When the carbon number of *n*-alkane was changed from 8 to 12, the phase diagram and X-point shifted to higher temperature and higher concentration of C_6E_2. Note that the area in three-phase in *n*-dodecane is larger than those in *n*-octane for all α examined in this work.

4. Conclusions

Fish-shaped diagrams for three ternary mixtures water + *n*-alkane + C_iE_j, i.e., water + *n*-octane + C_4E_1, water + *n*-octane + C_6E_2, and water + *n*-dodecane + C_6E_2, were determined using a cloud point method with a laser-scattering technique. X-points were also determined from the experimental cloud point data. Changes in the phase diagram and X-points with different *n*-alkane, C_iE_j, and the value of α were discussed from the experimental data. This experimental technique can be used for rapid and accurate determination of the fish-shaped diagram and X-point of SOW systems. It would also be useful for rapid determination of EACN for SOW systems based on temperature in the X-point.

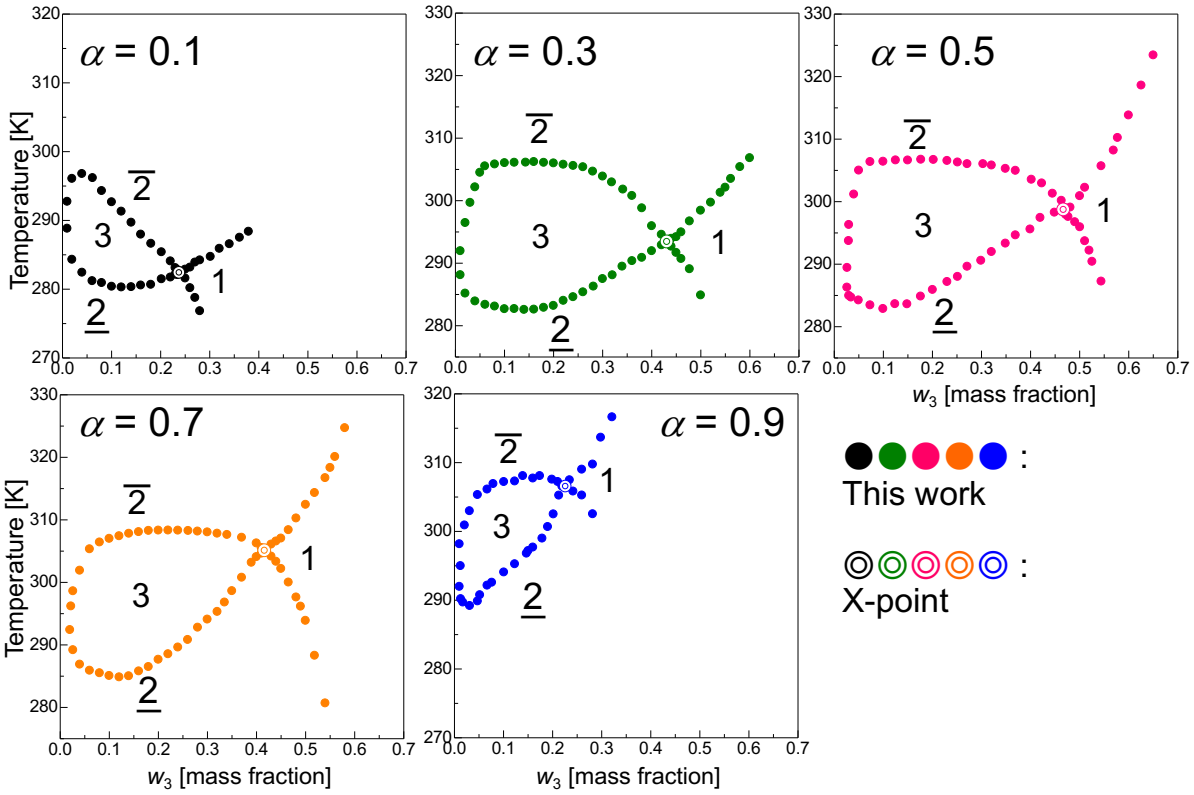

Fig. 8. Experimental fish-shaped diagram for the system water (1) + *n*-dodecane (2) + C_6E_2 (3).

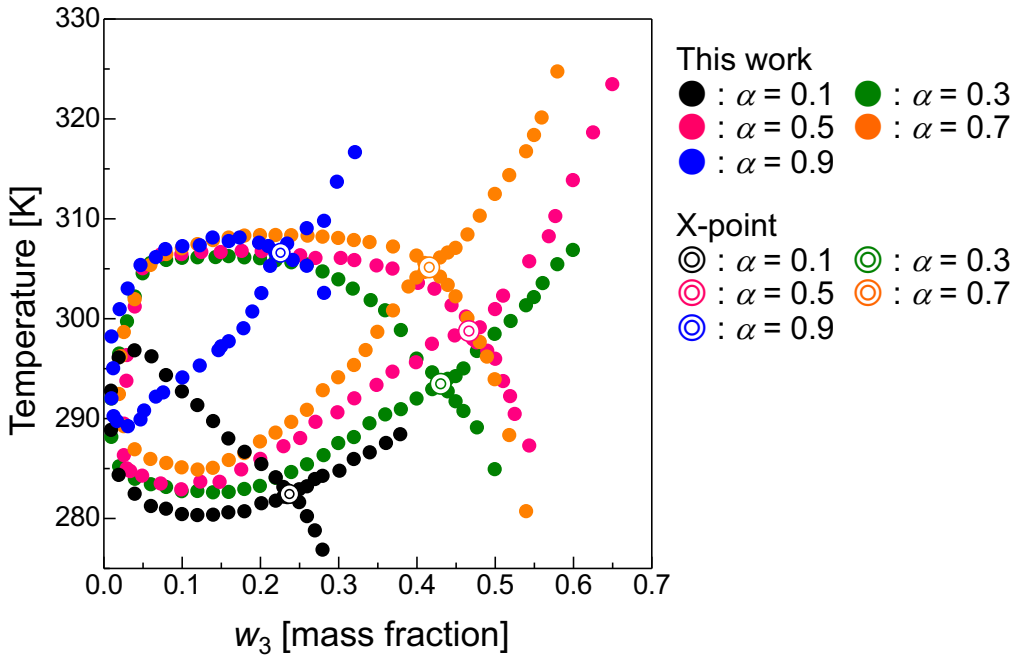

Fig. 9. Experimental fish-shaped diagram for the system water (1) + *n*-dodecane (2) + C_6E_2 (3).

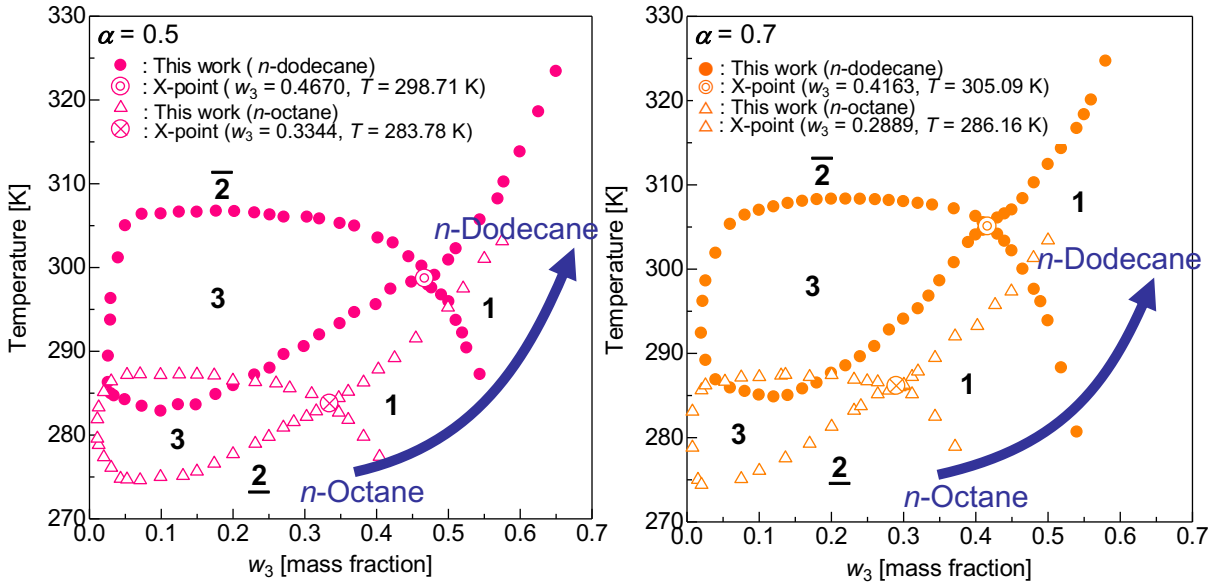

Fig. 10. Comparison of the experimental fish-shaped diagram for the systems water (1) + *n*-octane or *n*-dodecane (2) + C_6E_2 (3).

List of symbols

P	pressure (kPa)
T	absolute temperature (K)
w_i	liquid phase mass fraction of component i

Greek letters

ρ	density (kg m^{-3})

Superscripts

L	liquid
s	saturated

Subscripts

1, 2, 3, *i*, *j*	components 1, 2, 3, *i*, and *j*

References

[1] P. D. Fleming III, J. E. Vinatieri, J. Colloid Interface Sci. 81 (1981) 319-331.

[2] R. P. Frankewich, W. L. Hinze, Anal. Chem. 66 (1994) 944-954.

[3] J. G. Andersen, N. Koak, Th. W. de Loos, Fluid Phase Equilib. 163 (1999) 259-273.

[4] H. Kunieda, S. E. Friberg, Bull. Chem. Soc. Jpn. 54 (1981) 1010-1014.

[5] P. Winsor, Solvent Properties of Amphiphilic Compounds, Butterworth, London, 1954.

[6] W. H.Wade, J. C. Morgan, J. K. Jacobson, R. S. Schechter, Soc. Pet. Eng. J. 17 (1977) 122-128.

[7] S. Engelskirchen, N. Elsner, T. Sottmann, R. Strey, J. Colloid Interface Sci. 312 (2007) 114-121.

[8] V. Nardello, N. Chailloux, J. Poprawski, J.-L. Salager, J.-M. Aubry, Polym. Int. 52 (2003) 602-609.

[9] S. Queste, J. L. Salager, R. Strey, J. M. Aubry, J. Colloid Interface Sci. 312 (2007) 98-107.

[10] H. Kunieda, K. Shinoda, J. Colloid Interface Sci. 107 (1985) 107-121.

[11] J. F. Ontiveros, C. Pierlot, M. Catté, V. Molinier, A. Pizzino, J. -L. Salager, J. -M. Aubry, J. Colloid Interface Sci. 403 (2013) 67-76.

[12] F. Bouton, M. Durand, V. Nardello-Rataj, M. Serry, J. –M. Aubry, Colloids Surf. A 338 (2009) 142-147.

[13] F. Bouton, M. Durand, V. Nardello-Rataj, A. P. Borosy, C. Quellet, J. –M. Aubry, Langmuir 26 (2010) 7962-7970.

[14] M. Kahlweit, R. Strey, D. Haase, H. Kunieda, T. Schmeling, B. Faulhaber, M. Borkovec, H.-F. Eicke, G. Busse, F.Eggers, Th. Funck, H. Richmann, L. Magid, O. Söderman, P. Stilbs, J. Winkler, A. Dittrich, W. Jahn, J. Colloid Interface Sci. 118 (1987) 436-453

[15] C. L. Sassen, Th. W. de Loos, J. de Swaan Arons, J. Phys. Chem. 95 (1991) 10760-10763.

[16] C. L. Sassen, A. Gonzalez Casielles, Th. W. de Loos, J. de Swaan Arons, Fluid Phase Equilib. 72 (1992) 173-188.

[17] H. Hu, C. -D. Chiu, L.-J. Chen, Fluid Phase Equilib. 164 (1999) 187-194.

[18] Y. -L. Liu, D. -R. Chiou, L.-J. Chen, J. Chem. Eng. Data 47 (2002) 310-312.

[19] Y. -L. Liu, B. -J. Lin, L.-J. Chen, J. Chem. Eng. Data 48 (2003) 333-336.
[20] C. -H. Su, L. -J. Chen, J. Chem. Eng. Data 57 (2012) 1899-1902.
[21] C. -H. Su, L. -J. Chen, Fluid Phase Equilib. 346 (2013) 20-24.
[22] C. -H. Su, L. -J. Chen, Fluid Phase Equilib. 354 (2013) 75-79.
[23] S. -H. Chen, L. -J. Chen, Fluid Phase Equilib. 399 (2015) 16-21.
[24] K. Ochi, M. Tada, K. Kojima, Fluid Phase Equilib. 56 (1990) 341-359.
[25] K. Ochi, T. Saito, K. Kojima J. Chem. Eng. Data, 41 (1996) 361-364.
[26] K. Kurihara, T. Midorikawa, T. Hashimoto, K. Kojima, K. Ochi, J. Chem. Eng. Japan 35 (2002) 360-364.
[27] H. Matsuda, K. Kurihara, K. Ochi, K. Kojima, Fluid Phase Equilib. 203 (2002) 269-284.
[28] H. Matsuda, M. Fujita, K. Ochi, J. Chem. Eng. Data, 48 (2003) 1076-1080.
[29] H. Matsuda, D. Taniguchi, J. Hashimoto, K. Kurihara, K. Ochi, K. Kojima, Fluid Phase Equilib. 260 (2007) 81-86.
[30] H. Matsuda, A. Kitabatake, M. Kosuge, K. Kurihara, K. Tochigi, K. Ochi, Fluid Phase Equilib. 297 (2010) 187-191.
[31] K. Kurihara, Y. Yamanaka, H. Matsuda, K. Tochigi, K. Ochi, T. Furuya, Fluid Phase Equilib. 302 (2011) 110-115.
[32] H. Matsuda, Y. Hirota, K. Kurihara, K. Tochigi, K. Ochi, Fluid Phase Equilib. 357 (2013) 87-91.
[33] H. Matsuda, Y. Norizuki, M. Kawai, K. Kurihara, K. Tochigi, K. Ochi, J. Solution Chem. 43 (2014) 1561-1573.
[34] J. A. Riddick, W. Bunger, T. K. Sakano, Organic Solvents Physical Properties and Methods of Purification, 4th ed., John Wiley & Sons, New York, 1986.
[35] K. Shinoda, H. Sato, J. Colloid Interface Sci. 26 (1968) 70-74.